



EUROfusion

WPS1-CPR(18) 19502

J Zhu et al.

Multiphysics Analysis of W7-X Control Coils

Preprint of Paper to be submitted for publication in Proceeding of
30th Symposium on Fusion Technology (SOFT)



This work has been carried out within the framework of the EUROfusion Consortium and has received funding from the Euratom research and training programme 2014-2018 under grant agreement No 633053. The views and opinions expressed herein do not necessarily reflect those of the European Commission.

This document is intended for publication in the open literature. It is made available on the clear understanding that it may not be further circulated and extracts or references may not be published prior to publication of the original when applicable, or without the consent of the Publications Officer, EUROfusion Programme Management Unit, Culham Science Centre, Abingdon, Oxon, OX14 3DB, UK or e-mail Publications.Officer@euro-fusion.org

Enquiries about Copyright and reproduction should be addressed to the Publications Officer, EUROfusion Programme Management Unit, Culham Science Centre, Abingdon, Oxon, OX14 3DB, UK or e-mail Publications.Officer@euro-fusion.org

The contents of this preprint and all other EUROfusion Preprints, Reports and Conference Papers are available to view online free at <http://www.euro-fusionscipub.org>. This site has full search facilities and e-mail alert options. In the JET specific papers the diagrams contained within the PDFs on this site are hyperlinked

Multiphysics Analysis of W7-X Control Coils

Jiawu Zhu^{a,*}, Victor Bykov^a, Gunnar Ehrke^a, Boris Mendelevitch^b, Dirk Naujoks^a, Lutz Wegener^a, Hans-Stephan Bosch^a and W7-X team

^aMax-planck Institute for plasma physics, Greifswald, Germany

^bMax-planck Institute for plasma physics, Garching, Germany

The quasi-symmetric fivefold modular Wendelstein 7-X (W7-X) stellarator consists of three groups of coil systems, i.e. superconducting magnet, trim coil and control coil systems. The control coil system contains ten identical 3D shaped control coils (CC) situated behind the baffle plates of corresponding divertor units, and is designated to rectify the error field and to sweep hot spots on the divertor target plates. The CC is wound from copper conductor with a square cross section of 16 mm x 16 mm and a water cooling hollow of \varnothing 8 mm. The control coil system was installed in W7-X in 2015, and the integral commissioning has been done in parallel with the completion of W7-X. During the operation phase (OP 1.2a) with limited plasma heating energy, a leakage in one of the CC cooling water plug-in was found and dictates a detailed transient thermal analysis of CC to determine the allowable operation time without cooling water flow. The paper presents the transient thermal analysis and is followed by a detailed finite element mechanical analysis with the consideration of temperature gradient loads, dead weight and electromagnetic forces. Moreover, the transient thermal and mechanical performance of actively cooled CC to be intensively operated during steady state operation phase (OP 2) are also analyzed and evaluated with the same FE model.

Keywords: Wendelstein 7-X (W7-X), stellarator, control coil, thermal analysis, electromagnetic analysis, mechanical analysis.

1. Introduction

Following the successful first operation phase OP1.1 of the advanced modular stellarator Wendelstein 7-X (W7-X) with limiter plasma configurations, the second operation phases OP1.2a and OP1.2b with inertially cooled test divertor units (TDUs) are started in May of 2017 and April of 2018 respectively. The heating power of 8 MW in 10 s is limited by the TDUs and 2 TDU scraper elements, which are installed before OP1.2b for testing [1]. The control coil system, installed in W7-X in 2015, is also under commissioning during the second operation phase. It consists of ten identical 3D shaped control coils (CC) which are situated behind the baffle plates of corresponding divertor unit and designated to rectify the error field and to sweep hot spots on the divertor target plates [2-3]. Each CC winding pack comprises 8 turns (single pancake) of copper conductors, which are with a square cross section of 16 mm x 16 mm and a water cooling hollow of \varnothing 8 mm. Fig. 1 shows one of the CC resides in the divertor volume formed by graphite shielded baffle modules and divertor closures [4]. The CCs are fed with ten individual power suppliers and operated independently with a dc current and a superimposed ac current. The main parameters of one CC are listed in Table 1 [2].

The feed through for CC is inside a plug-in (see Fig. 1) and delivers cooling water and electrical current through two hollow conductors, it is connected with the CC conductor leads through well matched plugs and sealed with double O-rings. The connections are accomplished during the installation of CCs in 2015, however, a leakage is found in one of the connections during OP1.2a,

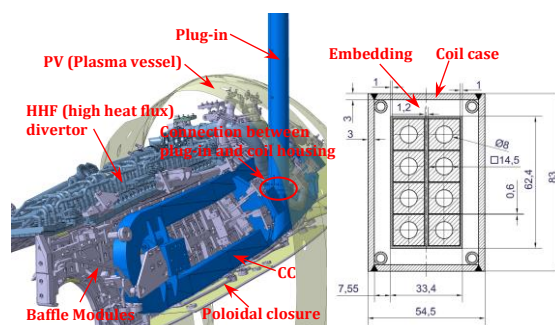


Fig. 1. View of one control coil situated inside of the divertor volume (part of PV is shown) and the coil section dimensions (unit: mm).

Table 1. Main parameters of one control coil

Designation	Value
Inductance	160 μ H
Resistance	3.95 m Ω
dc current	0 to \pm 2500 A
ac current	625 A _p
Max. eff. current	2539 A
Frequency of the ac current	0-20 Hz
Max. operation temperature	60 $^{\circ}$ C
Max. temperature baking	160 $^{\circ}$ C

which dictates a detailed transient thermal analysis of CC to determine the allowable operation time without cooling water flow. This paper at first studies the CC thermal behavior using a dedicated 3D FE model with the consideration of heat radiation, ohmic heating and ECRH (Electron-Cyclotron Resonance Heating), followed by the discussion and recommendation for CC operation. Secondly, the mechanical analysis with the

*Corresponding author. E-mail address: jiawu.zhu@ipp.mpg.de

consideration of temperature gradient loads, dead weight (DW) and Lorentz forces is presented and discussed. The Lorentz forces in CC are calculated using an electromagnetic (EM) model.

2. Transient Thermal Analysis

2.1 FE Model

As shown in Fig. 1, the control coil is surrounded by baffle modules (BM), TDU for OP1.2 or high heat flux (HHF) divertor for OP2, poloidal closure and plasma vessel (PV). The first wall elements are heated up during plasma operation [4]. As a result, radiant heat is concerned in CC thermal analysis, and realized by introducing a set of simplified FE model of the neighboring in-vessel components and PV (see Fig. 2).

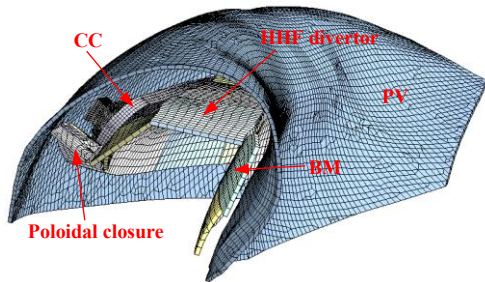


Fig. 2. FE model of simplified divertor volume for CC transient thermal analysis.

The CC inside the divertor volume is modeled with more details, as shown in Fig. 3, however the plug-in and feet through are excluded due to their negligible influences on thermal behavior. The 8 turns of conductor are modeled separately in simplified way, namely without the consideration of inter-turn and inter-pancake transitions. The most concerned CC winding pack (WP) is simulated with fine meshes with consideration of inter-turn, inter-layer and ground insulations. The insulations (glass fiber reinforced epoxy resin) are orthotropic materials which have different material properties in thickness direction and reinforcing plane specified in FE model by aligning the elements x coordinate direction with thickness direction (see Fig. 3c). The embedding fills the space between coil case and WP and is a mixture of ceramic sands (~ 50%) and epoxy resin. It is modeled as a isotropic material. Some bonded contacts are introduced to mimic the interfaces among WP, embedding, coil case and supports due to the inconsistency meshes. Four tubes at the corner of coil case (see Fig. 1) were temporary used for the epoxy resin impregnation, therefore they are excluded from FE modelling. The entire FE model comprises about 1.75 million nodes and 1.27 million elements generated in ANSYS Workbench 18.0®.

2.2 Scenarios for OP1.2

During OP1.2, the TDU, BM and poloidal closure are operated in a passive way which limits the plasma heating power to 8 MW at maximum, pulse length of ~10 s and dwell time between two pulses less than 20 min [1]. The CC are to be also operated during the same plasma pulses to perform required physics program.

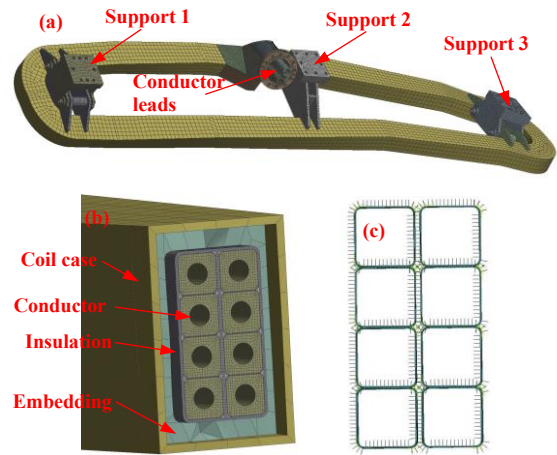


Fig. 3. FE model of 3D shaped control coil (a), mesh of coil section (b) and insulation elements orientation (c).

Consequently, the temperature of in-vessel components, as the boundary condition of thermal analysis, is also varied and substituted by the heat flux on plasma facing areas (for some analyzed cases) [5-7]:

- HHF divertor / TDU in high loaded area, 10 MW/m²,
- HHF divertor / TDU in low loaded area, 500 kW/m²,
- Baffle modules, 250 kW/m²,
- Poloidal closure, 100 kW/m².

The other parameters, such as emissivity, ECRH, heat generation, etc. of the analyzed scenarios are listed in Table 2. The temperatures of Case 1-3 are assumed for the scenario after 10 heating cycles according to the result of Case 1-1 and the calculation result reported in [6]. For conservative purpose, instead of 20 min the dwell time between two pulses is set to 10 min. The 380 W/m² ECRH load absorbed by stainless steel (SS) surfaces is the result of ~ 1 % absorption rate of the ECRH power of 38 kW/m² in divertor volumes of Module 1 or 5 [7]. The cooling water convection coefficient for OP1.2 (Case 1-4) is about 15.7 kW/m²·K (calculated according to the operation parameters presented in [8]), and the bulk temperature of coolant is set to 50 °C. The criteria for CC safe operation from thermal point of view including:

- Temperature difference in WP less than 40 °C in order to avoid considerable thermal stress,
- Maximum temperature in WP less than 150 °C (the temperature of baking).

Table 3 collects the analysis results of all cases. Fig. 4 shows the WP temperature at the end of two heating cycles of Case 1-1. For OP1.2 with passive cooling, it is clear that the WP temperature could meet the operation requirements only in the case when the CC is operated starting from initial cold state and heated during not more than two cycles. In case of operation after 10 cycles with the same initial condition (Case 1-3), the WP maximum temperature reaches 150 °C in 1160 s, and the temperature difference of 40 °C in 255 s. However, in case of water cooling (Case 1-4), the maximum temperature and temperature difference never reach the limits.

Table 2. Analysis scenarios and parameters of CC transient thermal analysis

Items		OP1.2				OP2	
		^a Case 1-1	^b Case 1-2	^c Case 1-3	^d Case 1-4	^e Case 2-1	^f Case 2-2
Time period, s		^g 604 x 2	604 x 2	604 x 4	604 x 2	250	1800
Temperature (°C) and emissivity	HHF TM5-6h	--, 0.9	--, 0.9	280, 0.9	--, 0.9	399.4, 0.2	399.4, 0.2
	HHF TM7-9h	--, 0.9	--, 0.9	900, 0.9	--, 0.9	145.5, 0.47	145.5, 0.47
	BM	--, 0.2	--, 0.2	180, 0.2	--, 0.2	317.5, 0.2	317.5, 0.2
	Poloidal closure	--, 0.5	--, 0.5	90, 0.5	--, 0.5	150, 0.5	150, 0.5
	PV	60, 0.5	60, 0.5	60, 0.5	60, 0.5	60, 0.5	60, 0.5
	Ambient Support	150	150	150	150	150	150
ECRH, W/m ²		^h 380	^h 380	^h 380	^h 380	380	380
Conductor heat generation, W/m ³		^h 4.428e6	^h 4.428e6	^h 4.428e6	^h 4.428e6	4.428e6	4.428e6

^aFor OP1.2, passive cooling.

^bFor OP1.2, with water in cooling path but not circulating.

^cFor OP1.2, assumed constant temperature of in-vessel component backside area after 10 heating cycles.

^dFor OP1.2, active cooling, ^eFor OP2, passive cooling, ^fFor OP2, active cooling.

^gTwo cycles, with 604 s per cycle, pulse length 10 s (including 2 s for heating power and current ramp up and down).

^hPulsed heating.

Table 3. Maximum temperature and temperature difference in CC WP

Cases (see Table 2)	Case 1-1	Case 1-2	Case 1-3	Case 1-4	Case 2-1	Case 2-2
Max. Temp. in WP during the solution time period, °C	79.3	74.4	238.3	63	184.5	62
Max. Δ Temp. in WP during the solution time period, °C	40	36.4	156	18	110	29
Time when Max. Temp. in WP reaching 150 °C, s	~2420*	~2720*	1160	Never*	175	Never*
Time when Max. Δ Temp. reaching 40 °C, s	1208	~1230*	255	Never*	47	Never*

*Estimated according to the analysis result.

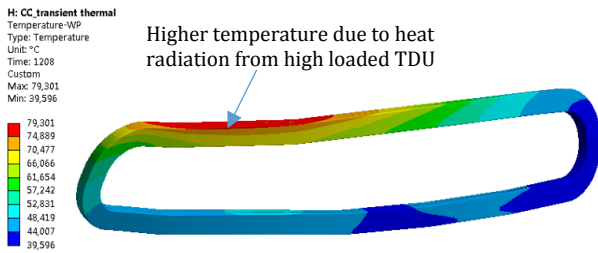


Fig. 4. Temperature distribution in WP at the end of two heating cycles of Case 1-1, °C.

2.3 Scenarios for OP2

The cooling water leakage issue is expected to be fully fixed before OP2, and the CC should be operated as designed in OP2. To verify the CC thermal performance during OP2, as listed in Table 2, two cases (passive and active cooling) are studied with the same FE model. The temperature and emissivity of in-vessel components backside area are set to the same values as the reference case of cryo-pump thermal analysis (with backside protection for BM and 25 % shading effect from neighboring pipelines) [9]. The cooling water convection coefficient (for Case 2-2) is about 280 kW/m²·K (calculated according to the operation parameters for OP2), and the bulk temperature of coolant is set to 50 °C.

As listed in Table 3, in case of passive cooling (Case 2-1) and start of CC operation from initial cold state, the CC WP is heated up rapidly to 150 °C (max. allowed temperature) in less than 3 min, and the state with temperature difference of 40 °C is reached in 47 s. However, as expected, the maximum temperature and temperature difference are always meet the requirements in case of active cooling (Case 2-2). As a result, active cooling of CC is considered as mandatory for OP2.

3. Mechanical Analysis

3.1 Electromagnetic forces

The superconducting (SC) magnet system of W7-X consists of 50 non-planar coils of 5 types and 20 planar coils of 2 types. The coils are toroidally arranged in five equal modules. Due to the strong magnetic field generated by SC coils and interacted with the CC currents, the EM forces in CC conductors are non-negligible for mechanical analysis. To be conservative, one of the reference EM regime named ‘low shear’ (LS) with 3.0 T average magnetic induction on plasma axis is selected for CC EM force calculation, and the CC current is set to 2500 A with exclusion of ac current component. The force calculation is performed with coupled-field solid elements (solid 5) in ANSYS. Due to the fact that external field is mainly in toroidal direction and almost parallel to the CC length direction, as shown in Fig. 6, EM forces in the CC middle part conductors are small, while the forces at the “ends” of CC are higher.

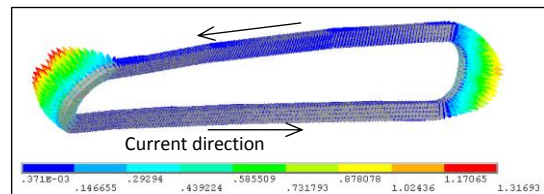


Fig. 6. EM forces in CC conductor elements, N.

3.2 Mechanical analysis

In addition to the EM forces, the DW and the temperature gradient from thermal analysis result of Case 1-1 and Case 2-2 are considered for mechanical analysis. The FE model is copied from thermal analysis with exception of the FE model parts of in-vessel components and PV, and with some modifications of

contacts, i.e. the bearing contacts of support 1 and 3 are changed to ‘frictional’ (friction factor of 0.12) to allow CC thermal expansion. In order to obtain the primary stress, the mechanical solution is separated into two steps:

- Step 1 with DW and EM forces, which are regarded as primary loads;
- Step 2 with additional temperature loads to introduce the thermal stress (secondary stress).

Table 4. Mechanical assessment of coil case and conductor

Case / Components	T, °C	^a P _m / limit, MPa	^b P _m +P _b / limit, MPa	^c P+Q / limit, MPa
Case 1-1, conductor	50	22.7/36.7	46.3/55	73.5/110
	50	26.8/36.7	31/55	40/110
Case 1-1, Coil case	60	*122/119	*180/178	164/355
	60	*137/119	154/178	138/355
Case 2-2, conductor	50	21.4/36.7	46.9/55	56.5/110
	50	25.4/36.7	28.6/55	32/110
Case 2-2, Coil case	50	*122/120	180/181	169/361
	50	*137/120	154/181	187/361

^aPrimary membrane stress

^bPrimary membrane plus bending stress

^cPrimary plus secondary stress

*Limits are low due to conservative yield stress from ITER

Table 5. Mechanical assessment of CC insulation

Stress / strain	Case 1-1	Case 2-2	Limits
Max. Comp. stress, MPa	142	115	800
Max. Pri. tensile strain, %	0.17	0.17	0.0
Max. Sec. tensile strain, %	0.095	0.15	0.02
Max. in-plane strain, %	0.33 ~	0.31 ~	± 0.5
Max. shear stress, MPa	2.1	2.0	56.7

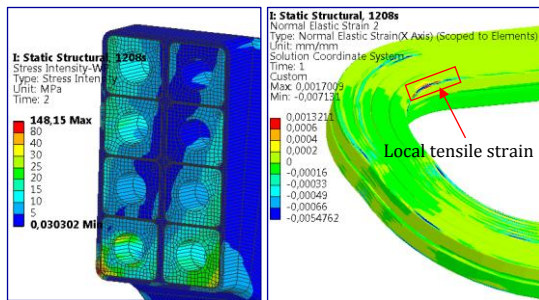


Fig. 7. Case 1-1, P+Q stress at WP cross section (left) and primary tensile strain in turn insulation (right).

According to the design criteria for ITER in-vessel components [10], The stress / strain limits for metallic and non-metallic structure assessment are defined and listed in Table 4 and 5 companying with the categorized stress / strain from the CC mechanical analysis. Two locations with high stress are identified for CC conductor / coil case assessment, as it is listed in Table 4. The primary loads for Case 1-1 and Case 2-2 are the same, but due to the temperature dependence of material properties, the P_m and P_m+P_b stresses are evaluated separately. Primary stresses slightly exceed the limits but only due to stress concentration, therefore, they are accepted. The assessment of CC insulation is listed in

Table 5. Some tensile strains in thickness direction exceed the limits, however, the criteria in the project are to accept such local delamination for coil insulation as it was done also for the trim coils. It is well visible in Fig. 7 that the maximum normal tensile strain in turn insulation (the issue of most concern) is really local, and the normal tensile strains are mostly lower than 0.02 %, therefore, the insulation mechanical behavior is also acceptable.

4. Conclusion

Transient thermal behavior of possible operation scenarios for control coils of W7-X is studied with a dedicated 3D FE model, which is capable to consider the heat radiation loads, ohmic heating and ECRH. According to the analysis results of the CC with active cooling, the CC thermal performance is excellent for both OP1.2 and OP2. However, in case of passive cooling, it is required to operate the CC only starting from cold state with not more than two heating cycles of 20 min during OP1.2. The operation without cooling during OP2 is not possible. Mechanical analysis of CC with the considerations of EM forces, dead weight and temperature gradient indicates that the mechanical performance of both metallic structure parts and non-metallic structure elements (insulation) of CC are acceptable.

Acknowledgment

This work has been carried out within the framework of the EUROfusion Consortium and has received funding from the Euratom research and training programme 2014-2018 under grant agreement No 633053. The views and opinions expressed herein do not necessarily reflect those of the European Commission.

References

- [1] H.-S. Bosch, T. Andreeva, et al., Engineering Challenges in W7-X: Lessons Learned and Status for the Second Operation Phase, IEEE Transactions on plasma science 46 (2018) 1131-1140.
- [2] F. Füllenbach, K. Risse et al., Commissioning of the Wendelstein 7-X in vessel control coil, IEEE Transactions on plasma science 46 (2018) 1131-1140.
- [3] F. Füllenbach, T. Rummel et al., Final test of the W7-X control coils power supply and its integration into the overall control environment, Fusion Eng. Des. 83 (2007) 1391-1395.
- [4] A. Peacock, J. Boscary, et al., Wendelstein 7-X High Heat Flux Components, IEEE 25th Symposium on Fusion Engineering, DOI: [10.1109/SOFE.2013.6635360](https://doi.org/10.1109/SOFE.2013.6635360).
- [5] M. Ye, 3D FE thermal & mechanical analysis of TDU, W7-X project document, PLM: 1-GXA50M-T0000.0
- [6] M. Ye, Thermal analysis of passive divertor target and in-vessel components, W7-X project document, PLM: 1-GXA-T0140.0.
- [7] R. Brakel, M. Köppen, A. Peacock, et al., Specification of Design Loads for in-vessel components of W7-X, W7-X project document, PLM: 1-AC-S0005.1.
- [8] M. Braun, Cooling configuration for control coil, W7-X project document, PLM: 1-ACK30-Z0002.4.

- [9] J. Zhu, V. Bykov, et al., Refined multiphysics analysis of W7-X cryopumps, IEEE Transactions on plasma science 46 (2018) 1592-1602.
- [10] ITER Structural design criteria for in-vessel components (SDC-IC), ITER, Cadarache, France.